catalysts

MDPI

Article

Carbamoyl-Decorated Cyclodextrins for Carbon Dioxide Adsorption

Vincenzo Patamia [1], Rosario Tomarchio [1], Roberto Fiorenza [2], Chiara Zagni [1], Salvatore Scirè [2], Giuseppe Floresta [1] and Antonio Rescifina [1,*]

[1] Department of Drug and Health Sciences, University of Catania, V.le A. Doria 6, 95125 Catania, Italy
[2] Department of Chemical Sciences, University of Catania, V.le A. Doria 6, 95125 Catania, Italy
* Correspondence: arescifina@unict.it

Abstract: Advances in materials science and technology have prompted researchers to look to nature for new high-performance, low-cost materials. Among these, cyclodextrins have been widely used as a material in industrial applications. Inspired by previous work by our research group that led to the functionalization of cucurbit[6]uryl and its conversion into supramolecular nanospheres with good CO_2 adsorption capacity, this work aims to improve the ability of cyclodextrins to capture CO_2 by functionalizing them with amide groups. Carbon dioxide adsorption experiments on functionalized cyclodextrins showed an adsorption capacity similar to that of BEA zeolite, a material currently used in the industry for gas adsorption. Moreover, these adsorption properties could also be exploited to improve the adsorption capacity of drugs, a field in which cyclodextrins are widely used. The new cyclodextrin molecules were characterized by nuclear magnetic resonance spectroscopy and mass spectrometry, thanks to which we could determine the degree of functionalization of the new macrocycles. In addition, using Fourier-transform infrared spectroscopy, we demonstrated the presence and interaction of carbon dioxide adsorbed by the material, whereas an in silico study confirmed the chemisorption as the principal adsorption process, as experimentally inferred using the pseudo-second-order (PSO) kinetic model.

Keywords: supramolecular chemistry; cyclodextrins; carbon dioxide adsorption; gas adsorption

check for updates

Citation: Patamia, V.; Tomarchio, R.; Fiorenza, R.; Zagni, C.; Scirè, S.; Floresta, G.; Rescifina, A. Carbamoyl-Decorated Cyclodextrins for Carbon Dioxide Adsorption. *Catalysts* **2023**, *13*, 41. https://doi.org/10.3390/catal13010041

Academic Editor: José R. B. Gomes

Received: 6 November 2022
Revised: 10 December 2022
Accepted: 20 December 2022
Published: 25 December 2022

Copyright: © 2022 by the authors. Licensee MDPI, Basel, Switzerland. This article is an open access article distributed under the terms and conditions of the Creative Commons Attribution (CC BY) license (https://creativecommons.org/licenses/by/4.0/).

1. Introduction

Cyclodextrins (CDs) are molecules with a cyclic structure, formally oligosaccharides of D-(+)-glucopyranosyl units linked by α-1,4-glycosidic bonds. Their main feature is a hydrophobic central cavity and a hydrophilic outer surface. Depending on D-(+)-glucopyranose units, the cavity can have different sizes. This attribute allows the CDs to form supramolecular complexes with hydrophobic guest molecules in water [1]. Due to the molecular complexation phenomena, CDs are widely used in many industrial and research fields. Among them are several analytical methods, environment protection, separation processes, drug carrier properties, fermentation, and catalysis. CDs have scrupulous substrate-binding ability and can catalyze various chemical reactions through reversible supramolecular interactions. There are several examples in the organic chemistry of reactions catalyzed by cyclodextrins. Our research group has recently employed CDs and other supramolecular structures in organic catalysis and supramolecular recognition of small organic compounds [2–7]. Inspired by our previous work, in which the functionalization of cucurbit[6]uril transformed it into a supramolecular nanosponge able to capture and reuse CO_2 [8], in this work, the supramolecular structure of CDs was the subject of the study to create a novel supramolecular structure able to sequestrate CO_2 from the environment.

The emission of greenhouse gases due to human activities and the resulting global warming have gained attention recently and will continue to increase. Increased carbon dioxide emissions is generally considered one of the leading causes of this human threat [9].

The response to this problem was initially centered on CO_2 capture technologies (membranes, adsorption, and absorption) [10,11]. Unfortunately, the conventional absorption processes have huge limitations and are sometimes economically inconvenient. For example, absorption based on alkanolamine aqueous solutions has high energy consumption and equipment corrosion rate. Moreover, membrane-based technologies are still not mature enough to be applied to industrial applications due to a still not mature technology. Consequently, CO_2 adsorption-based processes are currently promising approaches to overcome the limitations mentioned above. They are based on highly-efficient adsorbents, such as silicate materials, zeolite molecular sieves, and activated carbon [12–16].

CDs have shown promising results in the encapsulation and complexation of CO_2, and β-cyclodextrin (β-CD) has already been proven to form cyclodextrin-based nanosponges capable of capturing CO_2 gas [17,18]. Moreover, CDs have also been modified at their hydroxyl groups to improve CO_2 retention capabilities. For example, the primary face of β-CD was functionalized with an amino group showing excellent adsorption of CO_2/N_2 [19]. Considering the widespread use of systems functionalized with amide groups for carbon dioxide capture [19], we decided to use dimethylcarbamoyl chloride to carry out a simple and rapid functionalization of CDs, to obtain new amide-type derivative macrocycles and test them for CO_2 capture [20–23]. This work's novelty lies in indicating a simple and rapid functionalization strategy, employing the hydroxyl groups of the CD macrocycle, which can enable the development of a new, highly efficient material for CO_2 capture. This strategy avoids the long synthesis and separation processes used to date to prepare this type of material, going against green chemistry principles, which are gaining ground in academia and industry.

2. Results and Discussion

Scheme 1 reports the simple synthetic methodology to functionalize CDs using dimethylcarbamoyl chloride to increase the carbon dioxide adsorption capacity of macrocycles.

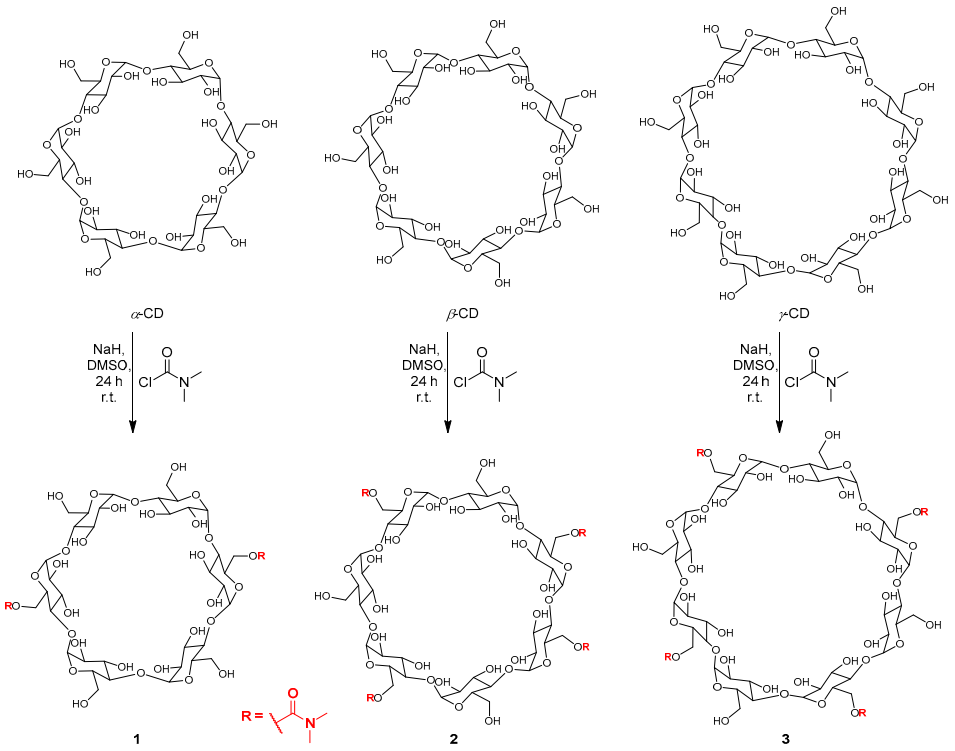

Scheme 1. Reaction scheme for the functionalization of CDs by dimethylcarbamoyl chloride. The positions of R groups are arbitrary.

The new CD carbamoyl derivates were then characterized through nuclear magnetic resonance spectroscopy (^{1}H and ^{13}C) and mass spectrometry (Figures S1–S15). The degree of functionalization of the new CDs was assessed from the NMR and mass data. Specifically, the di-functionalized macrocycle was found to be prevalent in compound **1**, whereas, for compounds **2** and **3**, the tetra-functionalized was the most abundant.

Figure 1 reports the comparison of the investigated CDs, the BEA zeolite (Zeolyst Int., CP 811-300 SiO_2/Al_2O_3 = 300, Brunauer–Emmett–Teller (BET) surface area 280 m^2/g), and our previous studied material based on cucurbit[6]uril (CB[6]-Funct) [8] (surface area 277 m^2/g). Interestingly, the functionalization of the α-CD exhibited the highest increase in the CO_2 capture (from q = 120.6 to q = 160.2), where q is the amount of carbon dioxide adsorbed calculated by the Equation (1),

$$Q\ (\mathrm{mg/g}) = [(C_{in} - C_f) \times t \times Q]/w, \quad (1)$$

where w is the weight of the examined sample (g), Q is the CO_2 flow rate (mL/min), t is the time (min) at which the saturation was achieved, and C_{in} and C_f are the initial and final (at the saturation) CO_2 concentrations (mg/mL), respectively [24]. The tests were carried out at room temperature and atmospheric pressure.

The modification of β-CD did not improve the sorption capacity (from q = 90.5 to q = 100.6), and only a slight enhancement was verified with the γ-CD (from q = 150.6 to q = 166.8). The functionalization of compound **1** allowed a better absorbent material than the BEA zeolite and the CB[6]-functionalized already reported. Since the BET surface areas of α-CD and **1** (32 m^2/g and 46 m^2/g) are lower than the benchmark samples, this improvement in CO_2 capture is not the result of an increased surface area. This behavior is instead related to the occurrence of the chemisorption of CO_2 favored by the specific functionalization.

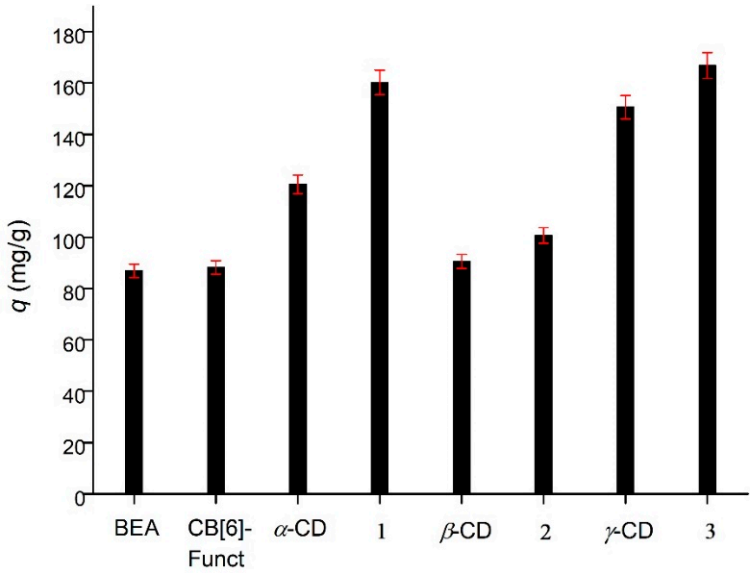

Figure 1. Quantification of CO_2 adsorption by the examined materials.

In addition to the direct comparison made in this work with the BEA and CB[6]-functionalized materials, to highlight the remarkable result obtained with the newly synthesized compounds for the carbon dioxide adsorption capacity, we report, in Table 1, a comparison with other widely used amides, according to the literature data.

Table 1. Comparison of CO_2 uptake abilities of amide-based materials.

Amide-Based Material	CO_2 Uptake (mg/g)	Reference
1	160.2	This work
2	100.6	This work
3	166.8	This work
BEA	87.2	This work
CB[6]-Funct	88.4	This work
PHTCZ-1	59.0	[25]
PHTCZ-2	103.0	[25]
M808-EDTA	64.2	[26]
MOF-1	44.0	[27]
MOF-2	43.6	[27]
MOF-3	82.3	[27]

From the comparison with MOFs and amide-based polymers, it can be deduced that the macrocycles we synthesized possess a higher CO_2 adsorption capacity. These results again emphasize that our easy and rapid synthetic methodology applied to CDs yields more than satisfactory results compared to the time-consuming and expensive methodologies reported for obtaining other materials.

Indeed, from the CO_2-TPD (temperature-programmed desorption) curve (Figure 2), it is possible to note that material **1** increased the desorption temperature by about 30 °C, pointing to a stronger interaction with CO_2 in the linear adsorptive form [28] compared to the unfunctionalized CD. These peaks could not be correlated to the thermal degradation of the α-CD structures, which were stable up to 300 °C [29].

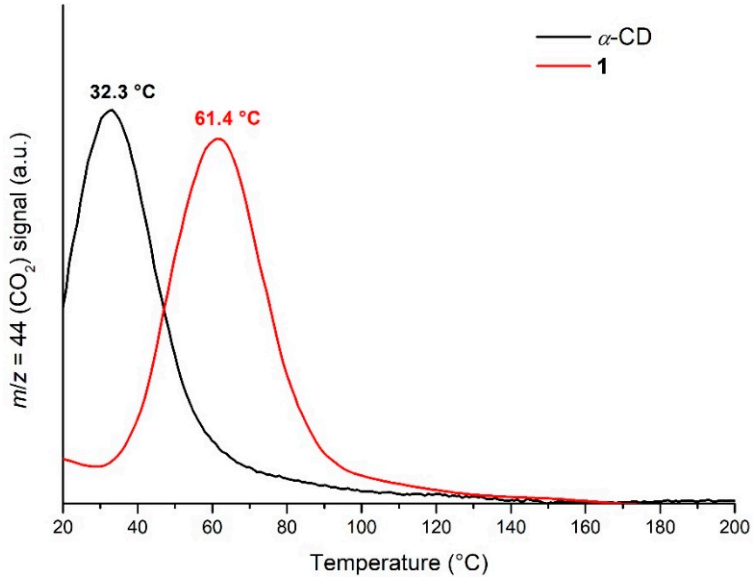

Figure 2. CO_2-TPD curves of the examined α-CD and **1** samples.

The α-CD and compound **1** samples showed an N_2 adsorption/desorption isotherm of type II, with an H3 hysteresis loop in the relative pressure (P/P_0) range of 0.9–1.0, typical of a macroporous structure (Figure S16) [30], along with a narrow pore size distribution centered at about 2 nm, calculated using the Barrett–Joyner–Halenda (BJH) method, and a pore volume of 0.06 cm^3/g, for both samples, according to the literature for similar CDs [31,32].

The kinetic measurements of CO_2 capture were performed on sample **1** and compared with the unmodified α-CD (Figure 3).

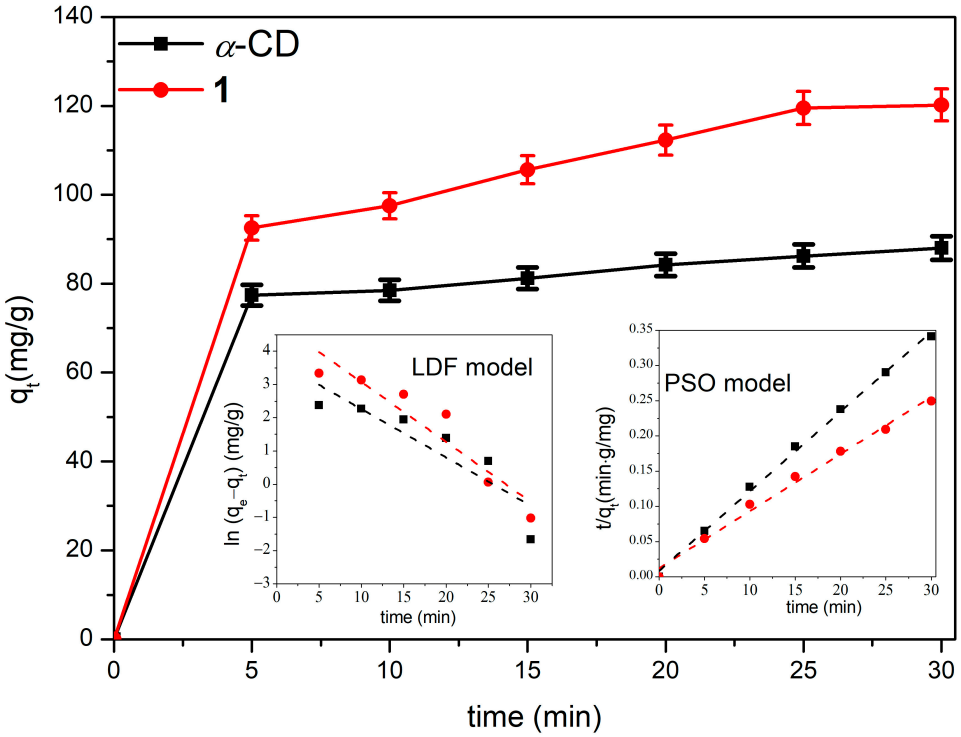

Figure 3. CO_2 capture kinetics on the samples of α-CD and **1**. In the insets, the experimental data (points) and the fit (dashed lines) with the LDF and the PSO models are shown.

According to the literature [33–35], the experimental data were fitted with the linear driving force (LDF) and the pseudo-second-order (PSO) models. These kinetic models are widely used for CO_2 adsorption kinetics [33,34,36].

The LDF model considers the adsorption rate proportional to the number of free surface sites suitable for the adsorption. The main driving force of the process is evaluated by the difference between the q at equilibrium and the q at the time t, whereas all the resistances due to the mass transfer are considered in the kinetic parameter k_t as global resistance to the diffusion, following Equation (2) (linear form).

$$\text{Ln}\,(q_e - q_t) = \ln q_e - k_t\, t, \tag{2}$$

where q_t and q_e were the amounts of CO_2 absorbed per unit mass of the sample at time t and at equilibrium, respectively.

On the contrary, the PSO model considers that the adsorption is dominated by the chemisorption between the CO_2 and the sample surface, following Equation (3).

$$t/q_t = (1/k_s\, q_e{}^2 + t/q_e), \tag{3}$$

where k_s is the adsorption rate constant.

From the data reported in Figure 3, it is evident that the PSO model fit well with the experimental data (R^2 = 0.99 for the samples examined), highlighting how chemisorption is the driving and dominant force of the process. Thus, the functionalization of compound **1** was found to be an essential chemical modification to favor the chemisorption of CO_2.

We also performed a differential scanning calorimetry (DSC) analysis to obtain information on the stability of compound **1** (Figure S17). The analysis shows that compound **1** probably started its degradation process at temperatures above 300 °C according to the information reported in the literature [37], which further emphasizes that it is an excellent candidate for the application under our study.

Focusing on α-CD, we performed infrared spectroscopy (IR) measurements of compound **1** to further validate that functionalization had occurred and to verify the CO_2

adsorption process. In Figure 4, we compare the IR spectra of α-CD and **1**, where typical vibrations were present. In particular, the absorption peaks at 3379, 2928, 1641, and 1029 cm^{-1} were attributed to O–H, C–H, C–C, and C–O–C stretching vibration of CD [38], respectively (black curve). In addition to these peaks, compound **1** (red curve) showed an absorption peak at 1695 cm^{-1}, which could be attributed to the vibration of the C=O (amide) inserted with the functionalization [39].

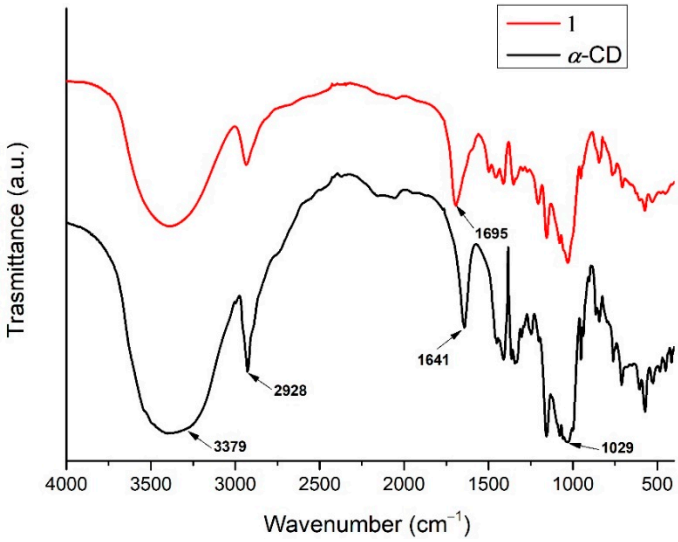

Figure 4. FTIR spectra of α-CD (black curve) and **1** (red curve).

To further verify the carbon dioxide adsorption process, an infrared spectroscopy measurement was carried out to compare **1** before and after CO_2 adsorption (Figure 5). The weak peak at 2345 cm^{-1} was the typical asymmetric stretching of the adsorbed CO_2 with the functionalized macrocycle [8,40–42]. It is possible to note that, in the IR spectrum of the **1** (red curve, before the CO_2 adsorption measurements), the peak related to CO_2 was absent.

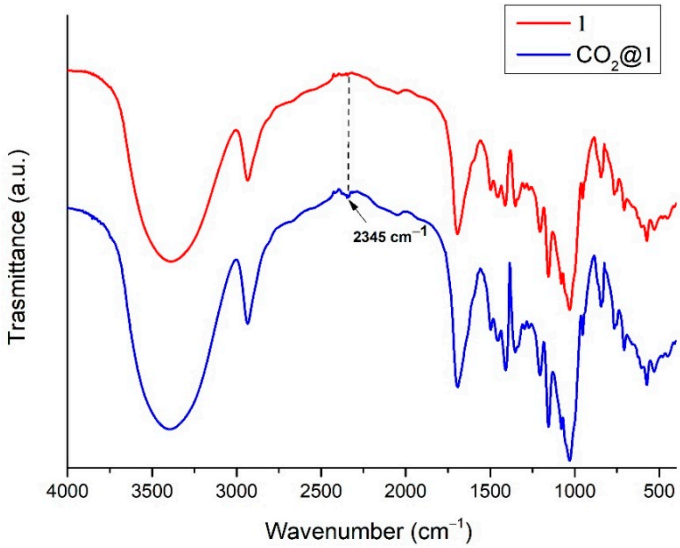

Figure 5. FTIR spectra of **1** before (red curve) and after (blue curve) CO_2 adsorption.

To shed light on the complex and the interactions between CO_2 and **1**, we performed an in silico study starting from a plausible model constituted by a dicarbamoyl substituted α-CD (at the O1 and O4 positions of the primary hydroxylic groups at the lower rim) with one molecule of CO_2 encapsulated in the hydrophobic cavity. After a metadynamics conformational sampling at the extended tight-binding level GFN2-xTB [43], the most stable

conformer was fully optimized at the DFT level of theory employing the M06-2X functional with the 6-31G(d) basis set, and a full natural bond orbital (NBO) analysis was performed. DFT calculation was performed using the Gaussian16 suite of programs [44]. Figure 6 shows the optimized 3D structure and selected NBOs. According to the second-order perturbation theory (SOPT) analysis, the stabilization energy between the two carbamoyl moieties and the CO_2 molecule was 18.8 kJ/mol, principally due to the $\pi \rightarrow \sigma^*$ and $\pi \rightarrow \pi^*$ interactions of the two carbamoylic C=O with the C–O and C=O of CO_2 (Figure 6, bottom); the total stabilization energy between the disubstituted α-CD and CO_2, from SOFT analysis was 80.6 kJ/mol and accounted for an adsorption process characterized by chemisorption [45], according to the experimental data. In this case, the extra stabilization energy due to the C=O carbamoyl interactions with CO_2 probably operated the switch between physisorption and chemisorption.

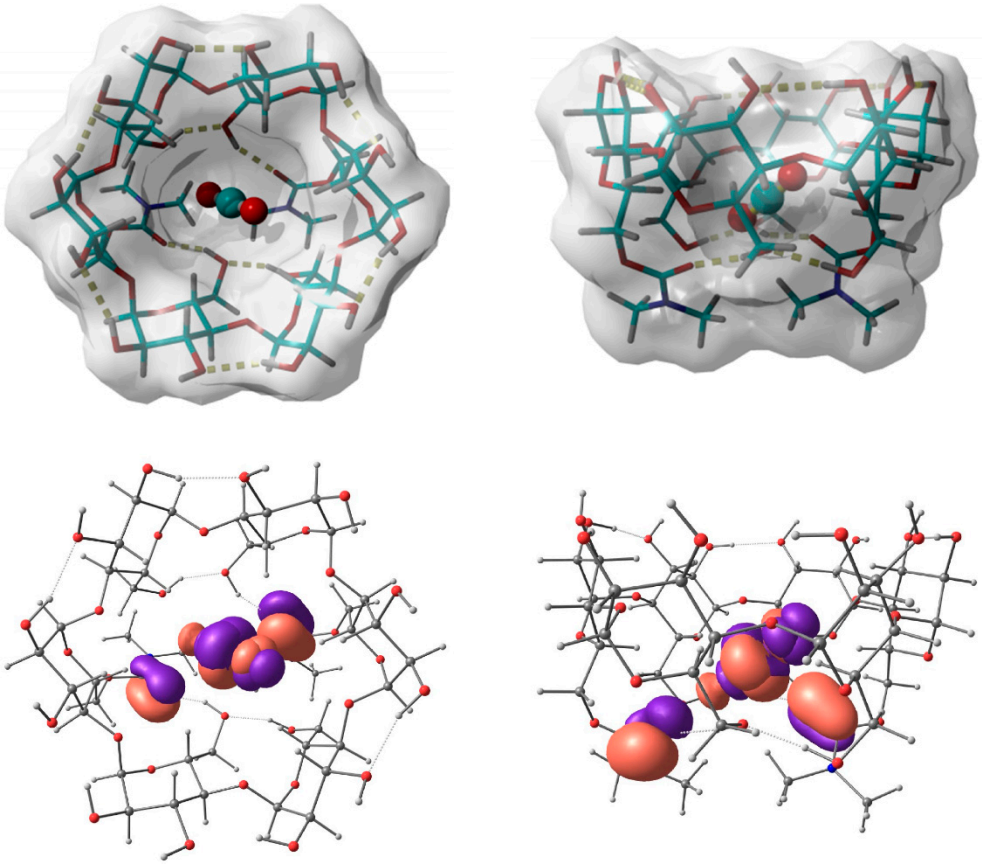

Figure 6. The 3D optimized molecular structure of the dicarbamoyl functionalized α-CD with one CO_2 molecule within the cavity. Top: front (left) and side (right) views with the molecular surface. Bottom: front (left) and side (right) views with the molecular orbital interactions.

The results clearly show that this simple procedure can be applied to functionalize CDs effectively and produce a material with good CO_2 adsorption properties. Furthermore, considering the excellent interaction between carbon dioxide and the functionalized CDs, one could consider reusing the CO_2 as a building block for synthesizing new molecules.

3. Materials and Methods

3.1. General Information

All the required chemicals were purchased from Merck: α-CD, β-CD, and γ-CD (>98.0%), dimethylcarbamoyl chloride (98%), sodium hydride in mineral oil (60%), acetone, and dimethyl sulfoxide anhydrous (DMSO) 99.9%. Precoated aluminum sheets (silica gel 60 F254, Merck) were used for thin-layer chromatography (TLC). ^{1}H- and ^{13}C-NMR spectra were recorded at 300 K on Varian UNITY Inova using DMSO-d_6 as the solvent at 500 MHz

for ^{1}H-NMR and 125 MHz for ^{13}C-NMR. ^{13}C spectra were ^{1}H-decoupled, and the APT pulse sequence determined the multiplicities. FTIR analyses in the 4000–400 cm^{-1} region were obtained using an FTIR System 2000 (Perkin-Elmer, Waltham, MA, USA) with KBr as the medium. MALDI mass spectra were acquired in reflector mode using a 4800 MALDI TOF/TOF™ Analyzer (Applied Biosystem, Framingham, MA, USA), equipped with a Nd:YAG laser (wavelength of 355 nm) and working in positive-ion mode.

The surface area determination was carried out using a Sorptomatic series 1990 instrument. The samples were pretreated with an outgassing step at 80 °C for 12 h, and the surface area was calculated using the BET method, while the pore size distribution was calculated using the BJH method.

For DSC analysis, the sample was accurately weighed (2.2 mg), crimped into aluminum trays, and heated from 50 to 320 °C at a heating rate of 10 °C/min in a nitrogen atmosphere using a Shimadzu DSC-60 device (Shimadzu, Kyoto, Japan). An empty, sealed aluminum tray was used as a reference.

3.2. General Procedure for the Synthesis of Carbamoyl-CDs Derivates 1–3

α-CD (0.4 g, 0.411 mmol) was dissolved in anhydrous DMSO (3 mL) in a round-bottom flask under nitrogen; NaH (230 mg, 5.76 mmol, 14 eq., 60% dispersion in mineral oil) was then added at 0 °C, and the reaction mixture was stirred for 1 h. After that, dimethylcarbamoyl chloride (530.33 µL, 5.76 mmol, 14 eq.) was added dropwise. The reaction was carried out for 24 h at r.t. with stirring. The reaction mixture was poured into acetone (25 mL), resulting in a pale-white solid precipitate that was collected by filtration, washed with acetone, and dried in the oven at 65 °C to give compound **1**. Yield = 66.44%. ^{1}H-NMR (500 MHz, DMSO-d_6): δ = 5.63–5.38 (m, 10H), 4.79 (s, 6H), 4.58–4.43 (m, 7H), 3.85–3.69 (m, 6H), 3.68–3.55 (m, 18H), 3.40–3.35 (m, 5H), 3.29–3.22 (m, 6H), 2.89 (s, 6H), 2.80 (s, 6H); ^{13}C-NMR (126 MHz, DMSO-d_6): δ = 155.45, 101.85, 82.09, 73.26, 72.07, 60.01, 35.78, 35.63, 30.77.

Synthesis of carbamoyl-*β*-CD (**2**): The title compound (white powder) was prepared analogously to compound **1**, using *β-CD* (0.4 g, 0.35 mmol), NaH (225.55 mg, 5.64 mmol, 16 eq., 60% dispersion in mineral oil), and dimethylcarbamoyl chloride (519.3 µL, 5.64 mmol, 16 eq.). Yield = 84.94%. ^{1}H-NMR (500 MHz, DMSO-d_6): δ = 5.92–5.69 (m, 13H), 4.83 (s, 7H), 4.57–4.47 (m, 8H), 3.73–3.52 (m, 38H), 2.89 (s, 12H), 2.80 (s, 12H); ^{13}C-NMR (126 MHz, DMSO-d_6): δ = 155.51, 101.87, 81.50, 80.86, 73.07, 72.43, 72.01, 60.26, 59.90, 36.14, 35.79.

Synthesis of carbamoyl-*γ*-CD (**3**): The title compound (white powder) was prepared analogously to compound **1**, using *γ-CD* (0.4 g, 0.31 mmol), NaH (222.51 mg, 5.64 mmol, 18 eq., 60% dispersion in mineral oil), and dimethylcarbamoyl chloride (515.6 µL, 5.64 mmol, 18 eq.). Yield = 89.69%. ^{1}H-NMR (500 MHz, DMSO-d_6): δ = 5.97–5.75 (m, 15H), 4.88 (s, 8H), 4.69–4.47 (m, 11H), 3.80–3.41 (m, 42H), 2.89 (s, 12H), 2.80 (s, 12H); ^{13}C-NMR (126 MHz, DMSO-d_6): δ = 155.55, 101.61, 80.87, 72.92, 72.62, 72.12, 59.94, 59.73, 36.12, 35.74.

3.3. CO_2 Adsorption and Desorption Experiments

The CO_2 capture measurements were performed in a quartz U-shaped reactor, utilizing 150 mg of the examined samples and a CO_2 (99.999%) flow of 30 mL/min. The CO_2 was detected using a quadrupole mass spectrometer (Sensorlab VG Quadrupoles) following the m/z = 44 signal. The adsorption of CO_2 was determined by measuring the ratio between the concentration of CO_2 after the saturation in the sample and the initial carbon dioxide concentration (i.e., without the sample). Before the measurements, the materials were pretreated in He flow (50 mL/min) at 100 °C for 1 h to remove eventual impurities from the surface of the sample. The amount of carbon dioxide adsorbed was calculated considering Equation (1).

The adsorption kinetic of CO_2 was measured using a thermogravimetric analyzer (Linseis STA PT 1600 instrument). The samples were degassed under a He stream (50 mL/min) at 100 °C for 1 h. When the experimental temperature was stabilized at 25 °C, the CO_2 was

fed into the test chamber with a flow rate of 30 mL/min, and the weight variation with time was recorded. The measurement error was within 3%. The CO_2-TPD tests were performed using 150 mg of sample in the same reactor. The CO_2 flow (30 mL/min) was stopped for these determinations after the adsorption and surface saturation processes. Subsequently, the reactor was heated from 20 °C to 200 °C (10 °C/min), following the $m/z = 44$ signal. In this case, the samples were also pretreated with a He flow (50 mL/min) for 1 h at 100 °C.

3.4. Computational Details

The 3D molecular structure of the model complex was submitted to a conformational search using CREST combined with the xTB at the semiempirical GFN2 level of theory. CREST employs an iterative conformational search workflow that generates conformer/rotamer ensembles through extensive metadynamic sampling, with an additional genetic z-matrix crossing step at the end. The most stable structure was utilized as the starting point for the DFT calculations.

4. Conclusions

Cyclodextrins are widely available, biodegradable molecules with optimal properties valuable for the design of novel materials. The two faces of the macrocycle can be selectively modified, thus enabling the preparation of several functionalized structures and providing easy access to multifunctional materials; moreover, CDs are compatible with several polymerization techniques. Carbamoyl-functionalized cyclodextrins have been synthesized to improve the CDs capacity to absorb CO_2. α-, β-, and γ-CD have been functionalized with an amide group to increase the CO_2 retention of the macrocycle. Among the different produced macrocycles, the α-CD functionalized material has been proven to be the most efficient. Carbon dioxide adsorption experiments showed that α-CD functionalized has an adsorption capacity similar to BEA zeolite, a material currently used in the industry for gas adsorption. The functionalization was proven by NMR and mass spectrometry, and the CO_2 adsorption was proven by IR and adsorption/desorption experiments. An in silico study confirmed chemisorption as the principal adsorption process. Furthermore, this concept could also be extended to improve the adsorption ability of drugs, a field in which cyclodextrins are widely exploited.

Supplementary Materials: The following supporting information can be downloaded at https://www.mdpi.com/article/10.3390/catal13010041/s1: Figure S1. ^{1}H NMR spectrum of **1**. Figure S2. ^{13}C NMR spectrum of **1**. Figure S3. ^{1}H NMR spectrum of α-CD. S4 Figure S4. ^{1}H NMR stacked spectra of α-CD and **1**. Figure S5. ^{1}H NMR spectrum of **2**. Figure S6. ^{13}C NMR spectrum of **2**. Figure S7. ^{1}H NMR spectrum of β-CD. Figure S8. ^{1}H NMR stacked spectra of β-CD and **2**. Figure S9. ^{1}H NMR spectrum of **3**. Figure S10. ^{13}C NMR spectrum of **3**. Figure S11. ^{1}H NMR spectrum of γ-CD. Figure S12. ^{1}H NMR stacked spectra of γ-CD and **3**. Figure S13. MALDI-TOF MS spectrum of compound **1**. Figure S14. MALDI-TOF MS spectrum of compound **2**. Figure S15. MALDI-TOF MS spectrum of compound **3**. Figure S16. N_2 adsorption-desorption isotherms and BJH pore size distribution of α-CD and **1**. Figure S17. DSC analysis of compound **1**.

Author Contributions: Conceptualization, V.P. and R.F.; methodology, G.F., R.T. and C.Z.; synthesis, R.T. and V.P.; validation, G.F., C.Z. and A.R.; formal analysis, V.P. and R.F.; investigation, V.P., R.T., R.F., C.Z. and G.F.; resources, S.S. and A.R.; data curation, V.P., C.Z. and G.F.; writing—original draft preparation, V.P., R.F. and G.F.; writing—review and editing, C.Z., S.S. and A.R.; supervision, G.F. and A.R.; project administration, S.S. and A.R. All authors have read and agreed to the published version of the manuscript.

Funding: This research received no external funding.

Data Availability Statement: Not applicable.

Conflicts of Interest: The authors declare no conflict of interest.

References

1. Del Valle, E.M.M. Cyclodextrins and their uses: A review. *Process Biochem.* **2004**, *39*, 1033–1046. [CrossRef]
2. Gambaro, S.; De Rosa, M.; Soriente, A.; Talotta, C.; Floresta, G.; Rescifina, A.; Gaeta, C.; Neri, P. A hexameric resorcinarene capsule as a hydrogen bonding catalyst in the conjugate addition of pyrroles and indoles to nitroalkenes. *Org. Chem. Front.* **2019**, *6*, 2339–2347. [CrossRef]
3. Floresta, G.; Talotta, C.; Gaeta, C.; De Rosa, M.; Chiacchio, U.; Neri, P.; Rescifina, A. γ-Cyclodextrin as a Catalyst for the Synthesis of 2-Methyl-3,5-diarylisoxazolidines in Water. *J. Org. Chem.* **2017**, *82*, 4631–4639. [CrossRef]
4. Loresta, G.; Rescifina, A. Metyrapone-β-cyclodextrin supramolecular interactions inferred by complementary spectroscopic/spectrometric and computational studies. *J. Mol. Struct.* **2019**, *1176*, 815–824. [CrossRef]
5. Gentile, D.; Floresta, G.; Patamia, V.; Nicosia, A.; Mineo, P.G.; Rescifina, A. Cucurbit[7]uril as a catalytic nanoreactor for one-pot synthesis of isoxazolidines in water. *Org. Biomol. Chem.* **2020**, *18*, 1194–1203. [CrossRef]
6. Floresta, G.; Punzo, F.; Rescifina, A. Supramolecular host-guest interactions of pseudoginsenoside F11 with β- and γ-cyclodextrin: Spectroscopic/spectrometric and computational studies. *J. Mol. Struct.* **2019**, *1195*, 387–394. [CrossRef]
7. Patamia, V.; Floresta, G.; Pistarà, V.; Rescifina, A. Green Efficient One-Pot Synthesis and Separation of Nitrones in Water Assisted by a Self-Assembled Nanoreactor. *Int. J. Mol. Sci.* **2022**, *23*, 236. [CrossRef] [PubMed]
8. Patamia, V.; Gentile, D.; Fiorenza, R.; Muccilli, V.; Mineo, P.G.; Scirè, S.; Rescifina, A. Nanosponges based on self-assembled starfish-shaped cucurbit[6]urils functionalized with imidazolium arms. *Chem. Commun.* **2021**, *57*, 3664–3667. [CrossRef]
9. Fleming, R.J. An updated review about carbon dioxide and climate change. *Environ. Earth Sci.* **2018**, *77*, 262. [CrossRef]
10. Ghiat, I.; Al-Ansari, T. A review of carbon capture and utilisation as a CO_2 abatement opportunity within the EWF nexus. *J. CO_2 Util.* **2021**, *45*, 101432. [CrossRef]
11. Vaz, S.; Rodrigues de Souza, A.P.; Lobo Baeta, B.E. Technologies for carbon dioxide capture: A review applied to energy sectors. *Clean. Eng. Technol.* **2022**, *8*, 100456. [CrossRef]
12. Siriwardane, R.V.; Shen, M.-S.; Fisher, E.P.; Poston, J.A. Adsorption of CO_2 on Molecular Sieves and Activated Carbon. *Energy Fuels* **2001**, *15*, 279–284. [CrossRef]
13. Wahby, A.; Silvestre-Albero, J.; Sepúlveda-Escribano, A.; Rodríguez-Reinoso, F. CO_2 adsorption on carbon molecular sieves. *Microporous Mesoporous Mater.* **2012**, *164*, 280–287. [CrossRef]
14. Silva, J.A.C.; Schumann, K.; Rodrigues, A.E. Sorption and kinetics of CO_2 and CH_4 in binderless beads of 13X zeolite. *Microporous Mesoporous Mater.* **2012**, *158*, 219–228. [CrossRef]
15. Wang, Y.; Memon, M.Z.; Seelro, M.A.; Fu, W.; Gao, Y.; Dong, Y.; Ji, G. A review of CO_2 sorbents for promoting hydrogen production in the sorption-enhanced steam reforming process. *Int. J. Hydrog. Energy* **2021**, *46*, 23358–23379. [CrossRef]
16. Elkhalifah, A.E.I.; Maitra, S.; Bustam, M.A.; Murugesan, T. Effects of exchanged ammonium cations on structure characteristics and CO_2 adsorption capacities of bentonite clay. *Appl. Clay Sci.* **2013**, *83–84*, 391–398. [CrossRef]
17. Trotta, F.; Cavalli, R.; Martina, K.; Biasizzo, M.; Vitillo, J.; Bordiga, S.; Vavia, P.; Ansari, K. Cyclodextrin nanosponges as effective gas carriers. *J. Incl. Phenom. Macrocycl. Chem.* **2011**, *71*, 189–194. [CrossRef]
18. Potluri, V.K.; Hamilton, A.D.; Karanikas, C.F.; Bane, S.E.; Xu, J.; Beckman, E.J.; Enick, R.M. The high CO_2-solubility of peracetylated α-, β-, and γ-cyclodextrin. *Fluid Phase Equilibria* **2003**, *211*, 211–217. [CrossRef]
19. Xu, L.; Xing, C.-Y.; Ke, D.; Chen, L.; Qiu, Z.-J.; Zeng, S.-L.; Li, B.-J.; Zhang, S. Amino-Functionalized β-Cyclodextrin to Construct Green Metal–Organic Framework Materials for CO_2 Capture. *ACS Appl. Mater. Interfaces* **2020**, *12*, 3032–3041. [CrossRef]
20. Moreau, F.; da Silva, I.; Al Smail, N.H.; Easun, T.L.; Savage, M.; Godfrey, H.G.W.; Parker, S.F.; Manuel, P.; Yang, S.; Schröder, M. Unravelling exceptional acetylene and carbon dioxide adsorption within a tetra-amide functionalized metal-organic framework. *Nat. Commun.* **2017**, *8*, 14085. [CrossRef]
21. Humby, J.D.; Benson, O.; Smith, G.L.; Argent, S.P.; da Silva, I.; Cheng, Y.; Rudić, S.; Manuel, P.; Frogley, M.D.; Cinque, G.; et al. Host–guest selectivity in a series of isoreticular metal–organic frameworks: Observation of acetylene-to-alkyne and carbon dioxide-to-amide interactions. *Chem. Sci.* **2019**, *10*, 1098–1106. [CrossRef] [PubMed]
22. Liu, H.-Y.; Gao, G.-M.; Bao, F.-L.; Wei, Y.-H.; Wang, H.-Y. Enhanced water stability and selective carbon dioxide adsorption of a soc-MOF with amide-functionalized linkers. *Polyhedron* **2019**, *160*, 207–212. [CrossRef]
23. Chen, M.; Chen, S.; Chen, W.; Lucier, B.E.G.; Zhang, Y.; Zheng, A.; Huang, Y. Analyzing Gas Adsorption in an Amide-Functionalized Metal Organic Framework: Are the Carbonyl or Amine Groups Responsible? *Chem. Mater.* **2018**, *30*, 3613–3617. [CrossRef]
24. Lu, C.; Bai, H.; Wu, B.; Su, F.; Hwang, J.F. Comparative Study of CO_2 Capture by Carbon Nanotubes, Activated Carbons, and Zeolites. *Energy Fuels* **2008**, *22*, 3050–3056. [CrossRef]
25. Sang, Y.; Cao, Y.; Wang, L.; Yan, W.; Chen, T.; Huang, J.; Liu, Y.-N. N-rich porous organic polymers based on Schiff base reaction for CO_2 capture and mercury (II) adsorption. *J. Colloid Interface Sci.* **2021**, *587*, 121–130. [CrossRef]
26. Park, J.M.; Yoo, D.K.; Jhung, S.H. Selective CO_2 adsorption over functionalized Zr-based metal organic framework under atmospheric or lower pressure: Contribution of functional groups to adsorption. *Chem. Eng. J.* **2020**, *402*, 126254. [CrossRef]
27. Lee, C.-H.; Wu, J.-Y.; Lee, G.-H.; Peng, S.-M.; Jiang, J.-C.; Lu, K.-L. Amide-containing zinc (II) metal–organic layered networks: A structure–CO_2 capture relationship. *Inorg. Chem. Front.* **2015**, *2*, 477–484. [CrossRef]

28. Fiorenza, R.; Bellardita, M.; Balsamo, S.A.; Spitaleri, L.; Gulino, A.; Condorelli, M.; D'Urso, L.; Scirè, S.; Palmisano, L. A solar photothermocatalytic approach for the CO_2 conversion: Investigation of different synergisms on CoO-CuO/brookite TiO_2-CeO_2 catalysts. *Chem. Eng. J.* **2022**, *428*, 131249. [CrossRef]
29. Bai, Y.; Wang, J.; Bashari, M.; Hu, X.; Feng, T.; Xu, X.; Jin, Z.; Tian, Y. A thermogravimetric analysis (TGA) method developed for estimating the stoichiometric ratio of solid-state α-cyclodextrin-based inclusion complexes. *Thermochim. Acta* **2012**, *541*, 62–69. [CrossRef]
30. Sing, K.S.W.; Everett, D.H.; Haul, R.A.W.; Moscou, L.; Pierotti, R.A.; Rouquerol, J.; Siemieniewska, T. Reporting physisorption data for gas/solid systems with special reference to the determination of surface area and porosity (Recommendations 1984). *Pure Appl. Chem.* **1985**, *57*, 603–619. [CrossRef]
31. Duman, O.; Polat, T.G.; Tunç, S. Development of poly(vinyl alcohol)/β-cyclodextrin/P(MVE-MA) composite nanofibers as effective and selective adsorbent and filtration material for the removal and separation of cationic dyes from water. *J. Environ. Manag.* **2022**, *322*, 116130. [CrossRef]
32. Martwong, E.; Chuetor, S.; Junthip, J. Adsorption of Paraquat by Poly(Vinyl Alcohol)-Cyclodextrin Nanosponges. *Polymers* **2021**, *13*, 4110. [CrossRef] [PubMed]
33. Stevens, L.; Williams, K.; Han, W.Y.; Drage, T.; Snape, C.; Wood, J.; Wang, J. Preparation and CO_2 adsorption of diamine modified montmorillonite via exfoliation grafting route. *Chem. Eng. J.* **2013**, *215*, 699–708. [CrossRef]
34. Gomez-Delgado, E.; Nunell, G.V.; Cukierman, A.L.; Bonelli, P.R. Influence of the carbonization atmosphere on the development of highly microporous adsorbents tailored to CO_2 capture. *J. Energy Inst.* **2022**, *102*, 184–189. [CrossRef]
35. Patamia, V.; Fiorenza, R.; Brullo, I.; Marsala, M.Z.; Balsamo, S.A.; Distefano, A.; Furneri, P.M.; Barbera, V.; Scirè, S.; Rescifina, A. A sustainable porous composite material based on loofah-halloysite for gas adsorption and drug delivery. *Mater. Chem. Front.* **2022**, *6*, 2233–2243. [CrossRef]
36. Ma, C.; Bai, J.; Hu, X.; Jiang, Z.; Wang, L. Nitrogen-doped porous carbons from polyacrylonitrile fiber as effective CO_2 adsorbents. *J. Environ. Sci.* **2023**, *125*, 533–543. [CrossRef]
37. Kaminski, K.; Adrjanowicz, K.; Kaminska, E.; Grzybowska, K.; Hawelek, L.; Paluch, M.; Tarnacka, M.; Gruszka, I.; Kasprzycka, A. Impact of water on molecular dynamics of amorphous α-, β-, and γ-cyclodextrins studied by dielectric spectroscopy. *Phys. Rev. E* **2012**, *86*, 031506. [CrossRef]
38. Xu, R.; Lin, X.; Xu, J.; Lei, C. Controlling the water absorption and improving the high C-rate stability: A coated Li-ion battery separator using β-cyclodextrin as binder. *Ionics* **2020**, *26*, 3359–3365. [CrossRef]
39. Larkin, P.J.; Makowski, M.P.; Colthup, N.B.; Flood, L.A. Vibrational analysis of some important group frequencies of melamine derivatives containing methoxymethyl, and carbamate substituents: Mechanical coupling of substituent vibrations with triazine ring modes. *Vib. Spectrosc.* **1998**, *17*, 53–72. [CrossRef]
40. Neoh, T.-L.; Yoshii, H.; Furuta, T. Encapsulation and Release Characteristics of Carbon Dioxide in a-Cyclodextrin. *J. Incl. Phenom. Macroc. Chem.* **2006**, *56*, 125–133. [CrossRef]
41. Ho, T.M.; Howes, T.; Bhandari, B.R. Encapsulation of CO_2 into amorphous and crystalline α-cyclodextrin powders and the characterization of the complexes formed. *Food Chem.* **2015**, *187*, 407–415. [CrossRef]
42. Ho, T.M.; Tuyen, T.; Howes, T.; Bhandari, B.R. Method of Measurement of CO_2 Adsorbed into α-Cyclodextrin by Infra-Red CO_2 Probe. *Int. J. Food Prop.* **2016**, *19*, 1696–1707. [CrossRef]
43. Pracht, P.; Bohle, F.; Grimme, S. Automated exploration of the low-energy chemical space with fast quantum chemical methods. *Phys. Chem. Chem. Phys.* **2020**, *22*, 7169–7192. [CrossRef] [PubMed]
44. Frisch, M.J.; Trucks, G.W.; Schlegel, H.B.; Scuseria, G.E.; Robb, M.A.; Cheeseman, J.R.; Scalmani, G.; Barone, V.; Mennucci, B.; Petersson, G.A.; et al. *Gaussian 16 Revision C.01*; Gaussian, Inc.: Wallingford, CT, USA, 2016.
45. Berger, A.H.; Bhown, A.S. Comparing Physisorption and Chemisorption Solid Sorbents for use Separating CO_2 from Flue Gas using Temperature Swing Adsorption. *Int. Conf. Greenh. Gas Control. Technol.* **2011**, *4*, 562–567. [CrossRef]

Disclaimer/Publisher's Note: The statements, opinions and data contained in all publications are solely those of the individual author(s) and contributor(s) and not of MDPI and/or the editor(s). MDPI and/or the editor(s) disclaim responsibility for any injury to people or property resulting from any ideas, methods, instructions or products referred to in the content.